

Finite temperature properties of the $SO(3)$ lattice gauge theory

Srinath Cheluvareja*

Tata Institute of Fundamental Research, Mumbai 400 005, India

H. S. Sharatchandra†

The Institute of Mathematical Sciences, Madras - 600 113, India

(Received 8 October 1998; published 2 May 2000)

We make a numerical study of the finite temperature properties of the $SO(3)$ lattice gauge theory. As its symmetry properties are quite different from those of the $SU(2)$ LGT, a different set of observables has to be considered in this model. We study several observables, such as the plaquette square, the $Z(2)$ monopole density, the fundamental and adjoint Wilson line, and the tiled Wilson line correlation function. Our simulations show that the $Z(2)$ monopoles condense at strong coupling just as in the bulk system. This transition is seen at approximately the same location as in the bulk system. A surprising observation is the multiple valuedness of the adjoint Wilson line at high temperatures. At high temperatures, we observe long lived metastable states in which the adjoint Wilson line takes positive and negative values. The numerical values of other observables in these two states appear to be almost the same. We study these states using different methods and also make comparisons with the high temperature behavior of the $SU(2)$ LGT. Finally, we discuss various interpretations of our results and point out their relevance for the phase diagram of the $SO(3)$ LGT at finite temperature.

PACS number(s): 12.38.Gc, 05.70.Fh, 11.15.Ha

I. INTRODUCTION

Lattice gauge theories (LGTs) at non-zero temperatures have been studied extensively for many years. They have provided us with models for the confinement-deconfinement phase transition which is expected to occur in realistic theories such as quantum chromodynamics. The thermodynamic properties of the $SU(2)$ and $SU(3)$ LGTs have also been vigorously studied [1]. Nevertheless, the implications of LGTs for continuum Yang-Mills theories are not completely clear. There are many questions about the high temperature phase which have still eluded an understanding; some of these are a precise characterization of the phase, the structure of its elementary excitations, and its static and dynamic properties. This makes the study of the finite temperature properties of LGTs a subject of continuing interest.

The pioneering work in [2] was the first non-perturbative calculation to show that quarks are deconfined at high temperatures. The analysis in [2] is done in the strong coupling limit ($g \gg 1$) of the $SU(2)$ LGT. In this limit, the partition function of the $SU(2)$ LGT is rewritten as a 3D spin model with a global $Z(2)$ symmetry. The ordered phase of this spin model corresponds to the deconfined phase and the disordered phase corresponds to the confined phase. Following this calculation, Monte Carlo simulations [3] provided further evidence that the transition takes place in the physical weak coupling limit ($g \ll 1$). These simulations are usually done [for the $SU(2)$ LGT] using the Wilson action [4] which is defined as

$$S = \frac{\beta_f}{2} \sum_{n, \mu < \nu} \text{tr}_f U(n, \mu \nu). \quad (1)$$

The $U(n, \mu \nu)$ s are the plaquette variables that are the oriented product of the $SU(2)$ link variables along an elementary square and are constructed as

$$U(n, \mu \nu) = U(n, \mu) U(n + \mu, \nu) U^\dagger(n + \nu, \mu) U^\dagger(n, \nu). \quad (2)$$

$U(n, \mu)$ are the $SU(2)$ variables defined on the links. The basic observable that is studied in simulations is the Wilson-Polyakov line (henceforth called the Wilson line); this is defined as

$$L_f(x) = \text{Tr}_f P \exp \left(i \int_0^\beta A(x) dx_4 \right). \quad (3)$$

The subscript f indicates that the trace is taken in the fundamental representation of the group. In analogy with the Wilson loop, the expectation value of this observable can be interpreted as the free energy of a static quark in a heat bath (at a temperature β^{-1}). This connection is made explicit by writing it in the form

$$\langle L_f(x) \rangle = \exp[-\beta F(x)]. \quad (4)$$

A non-zero expectation value of the Wilson line signals deconfinement; a zero expectation value signals confinement. This observable is the order parameter for studying the confinement-deconfinement phase transition in $SU(N)$ LGTs. The importance of the center of the gauge group, $Z(N)$ for $SU(N)$, was further underlined in [5] where it was proposed that the critical behavior of 4D $SU(N)$ gauge theories could be understood in terms of the critical behavior of 3D spin models having a global $Z(N)$ symmetry. The group $Z(N)$, which is the center of the group $SU(N)$, plays a special role in the deconfinement transition. This is because of an extra symmetry in the finite temperature gauge theory that arises from the periodic boundary conditions in the Euclid-

*Email address: srinath@theory.tifr.res.in

†Email address: sharat@imsc.ernet.in

ean time direction; gauge transformations which are periodic (in time) up to a constant center element leave the action invariant. The Wilson line picks up a phase under the action of these gauge transformations; it transforms as

$$L_f(x) \rightarrow ZL_f(x); \quad (5)$$

here Z is an element of the center and, for the group $SU(2)$, it is either $+1$ or -1 . Therefore, a non-zero value of the Wilson line at high temperatures signals a spontaneous breaking of the global center symmetry, implying that the high temperature phase is degenerate with the two degenerate states related by a Z transformation. Numerical simulations of the $SU(2)$ LGT observe these degenerate states as metastable states in simulations. At high temperatures, the Wilson line settles to either a positive or a negative value and remains in either of these two states for very long simulation times. The order of the transition to the high temperature phase has also been investigated thoroughly in the $SU(2)$ and the $SU(3)$ LGTs. The expectations in [5], concerning the order of the phase transition, have been borne out for the $SU(2)$ [6] and the $SU(3)$ [7] LGTs in which one observes a 3D Ising like critical behavior and a 3D $Z(3)$ like first order transition respectively.

Since lattice actions are anyway not unique, it is natural to study the finite temperature properties of LGTs using equivalent actions. The universality of lattice gauge theory actions requires that different actions, which correspond to different regularizations of quantum field theories, should reproduce the same physics in the continuum limit. One such LGT is defined by

$$S = \frac{\beta_a}{3} \sum_p \text{tr}_a U(p). \quad (6)$$

Unlike the Wilson action, the trace of the plaquette is taken in the adjoint representation. The traces in the two representations are related by

$$\text{tr}_a U = (\text{tr}_f U)^2 - 1. \quad (7)$$

Though this action is defined using $SU(2)$ link variables and the $SU(2)$ Haar measure, it describes an $SO(3)$ LGT because the link variables $U(n, \mu)$ and $-U(n, \mu)$ have the same weight. In this paper, we will report on our studies with this action and we will encounter some unexpected and interesting phenomena.

There are several reasons why a study of the finite temperature properties of the $SO(3)$ LGT can be useful and important. The $SO(3)$ LGT has the same naive continuum limit as the $SU(2)$ LGT, and is expected to lead to the same physics as the $SU(2)$ LGT. Furthermore, since the group $SO(3)$ has no non-trivial center subgroup like $SU(2)$, it would be interesting to see how it can reproduce the same properties as the $SU(2)$ LGT in the absence of a non-trivial center subgroup. Also, unlike the $SU(2)$ LGT, the $SO(3)$ LGT has a first order bulk transition at $\beta_a \approx 2.6$ that is driven by the condensation of $Z(2)$ monopoles [8]. The condensation of these $Z(2)$ monopoles has nothing to do with deconfinement. Both sides of the bulk transition are confining

phases, and only the $Z(2)$ degrees of freedom behave differently in these two phases. The presence of these additional $Z(2)$ degrees of freedom should lead to a richer phase diagram in which both sides undergo phase transitions into a high temperature phase. Another issue which has been discussed recently is the difficulty in separating a bulk and a finite temperature transition. The finite temperature properties of the mixed action $SU(2)$ LGT (introduced in [9]) were recently studied in [10] and it was found that the deconfinement transition joined the bulk transition, making it difficult to separate the two. This raises the issue of whether it is possible to make any meaningful distinction between these two transitions. Similar studies have also been made with a mixed action $SU(3)$ LGT in [11]. It is with these motivations in mind that we have tried to understand the finite temperature properties of the $SO(3)$ LGT. The Monte Carlo simulation method is used to arrive at the numerical results. We run into many puzzling features in our studies of the $SO(3)$ LGT. Our studies indicate that the $SO(3)$ LGT has a much richer behavior than the $SU(2)$ LGT. In this paper we first present our numerical observations and later make proposals for their physical interpretation. We consider different scenarios for the phase diagram of the $SO(3)$ LGT. Though we do not have a convincing proof for any particular scenario, we present several reasons for favoring the scenario that we believe is true.

We first observe that the Wilson line in the fundamental representation is not an order parameter in the $SO(3)$ LGT. This is because the global $Z(2)$ symmetry present in the $SU(2)$ LGT is promoted to a local symmetry in the $SO(3)$ LGT. The center transformation can now depend on the spatial position and acts as

$$\mathbb{L}_f(x) \rightarrow Z(x)\mathbb{L}_f(x). \quad (8)$$

Since local symmetries are never spontaneously broken [12], this forces the average value of the Wilson line in the fundamental representation to be always zero. Only observables which are invariant under this local symmetry can have a non-zero average value in this model. Before we discuss these observables, it is illuminating to rewrite the action for the $SO(3)$ LGT in a slightly different form. This involves linearizing the square term of the trace by introducing an auxiliary Gaussian field $[\lambda(p)]$ on the plaquettes, after which the action becomes

$$S = \frac{\sqrt{\beta_a}}{\sqrt{3}} \sum_p \text{tr}_f U(p) \lambda(p) - \frac{1}{4} \sum_p \lambda(p)^2. \quad (9)$$

In the above form, the $SO(3)$ LGT is like an $SU(2)$ LGT interacting with additional Gaussian plaquette degrees of freedom. These plaquette variables are the $Z(2)$ degrees of freedom. This form also shows that the $SO(3)$ LGT has additional degrees of freedom compared with the $SU(2)$ LGT. The $SU(2)$ LGT is recovered when the additional $Z(2)$ variables are frozen to $+1$. The above form of the action, unlike the form in Eq. (6), is also convenient for

simulations for which a heat bath or an overrelaxation algorithm has to be implemented. The action has the local $Z(2)$ invariance

$$U(n, \mu) \rightarrow -U(n, \mu) \quad \lambda(p) \rightarrow -\lambda(p), \quad (10)$$

the $\lambda(p)$ s being the plaquettes touching the link $U(n, \mu)$. To study this model, we must construct observables that are invariant under these local gauge transformations. Wilson loops and Wilson-Polyakov lines fail to satisfy this criterion and their average values are identically zero. Nevertheless, we can discuss the behavior of several observables which are invariant under these local gauge transformations. One such observable is a sheet variable. An example of a sheet variable is the ‘‘tiled’’ Wilson loop

$$W(C) = \prod_{l \in C} U(l) \prod_{p \in C} \lambda(p). \quad (11)$$

The first part of the observable is the usual Wilson loop defined over a loop C , and the other part consists of the auxiliary $Z(2)$ variables which are defined on all the plaquettes enclosed by the loop C . The tiled Wilson loop cannot be given the usual physical interpretation of the potential of a quark-antiquark pair because additional $Z(2)$ degrees of freedom are involved in its definition. Nevertheless, it is an interesting gauge invariant variable that incorporates both the $SU(2)$ and the $Z(2)$ degrees of freedom in the $SO(3)$ LGT. Similarly, we can define a ‘‘tiled’’ Wilson line correlation function as

$$W(x, y) = \text{tr} L_f(x) L_f(y) \prod_{p \in C} \lambda(p). \quad (12)$$

We expect this observable to be useful in studying the finite temperature properties of the $SO(3)$ LGT. The $Z(2)$ monopole density, ρ , can be extracted from the $\lambda(p)$ variables as follows:

$$\rho(c) = \frac{1}{2} \left[1 - \text{sgn} \left(\prod_{p \in \partial c} \lambda(p) \right) \right]. \quad (13)$$

This definition of the monopole density is also gauge invariant. By definition, a $Z(2)$ monopole is present in a 3D cube whenever the product of the $Z(2)$ auxiliary variables bordering the cube is negative. The $Z(2)$ monopoles can be imagined as lattice monopole configurations that carry a net $Z(2)$ magnetic flux. Another observable of interest is the Wilson line in the adjoint representation that is defined as

$$L_a(x) = \text{Tr}_a P \exp \left(i \int_0^\beta A(x) dx_4 \right). \quad (14)$$

This observable can also be studied in the $SU(2)$ [13–15] and the $SU(3)$ [16] LGTs at finite temperature, and it can be used to monitor the deconfinement transition. However, the adjoint Wilson line plays a much more essential role in the study of deconfinement in the $SO(3)$ LGT. For the group $SU(2)$, this observable can be expressed in terms of the fundamental Wilson line L_f by the relation

$$L_a = L_f^2 - 1. \quad (15)$$

In this form, it is easy to see that the adjoint Wilson line is invariant under the local $Z(2)$ transformation in Eq. (8) and is in general non-zero. In analogy with the fundamental Wilson line in the $SU(2)$ LGT, we expect the adjoint Wilson line to tell us something about the deconfinement transition in the $SO(3)$ LGT. The physical interpretation attached to the fundamental Wilson line carries over to the adjoint Wilson line. It measures the free energy of a static source (F_a) in the adjoint representation placed inside a heat bath at a temperature β^{-1} . This is again seen by writing it as

$$\langle L_a(x) \rangle = \exp[-\beta F_a(x)]. \quad (16)$$

A non-zero value of this observable implies that such a static source has a finite free energy. It must be noted, however, that confinement of adjoint sources is to be understood slightly differently from confinement of fundamental sources. An adjoint source [which is a non-Abelian charge in the $j=1$ representation of $SU(2)$] can always bind with two fundamental sources ($j=1/2$) and form a color singlet bound state. Similarly, two widely separated adjoint sources will form two color singlet bound states without any string joining the two. Hence, unlike the fundamental Wilson line, the adjoint Wilson line is always non-zero, and it is not an order parameter in the strict sense. Nevertheless, it can show discontinuous behavior across a phase transition just like any other observable. Since the behavior of an adjoint source depends on its ability to bind to fundamental sources, we expect the adjoint source to closely follow the behavior of fundamental sources. This is true for the $SU(2)$ LGT in which the adjoint Wilson line can equally well be used to locate the deconfinement transition. Finally, the other gauge invariant variable we consider is the square of the plaquette variable defined as

$$P = (1/3) \text{tr} U(p)^2. \quad (17)$$

This measures the energy density in a bulk system.

In the next section we present our numerical studies of the above-mentioned observables, and then we attempt to provide a physical interpretation to our results.

II. NUMERICAL RESULTS

In this section we present our numerical results. We first briefly describe the systematics of the simulation. A metropolis update (with 3 hits) followed by overrelaxation updates (2 hits) was used to generate the configurations. Measurements were made every 10 sweeps after omitting the first 1000 configurations. We performed runs ranging from 10000 to 50000 Monte Carlo sweeps. The link variables and the Gaussian variables were updated separately. Since any simulation should also incorporate the local invariance in Eq. (10), the transformations in Eq. (10) were implemented every time a measurement was made. This is done by randomly changing the sign of a link variable and simultaneously changing the signs of all the auxiliary variables which are in contact with this link. This process is repeated until it has

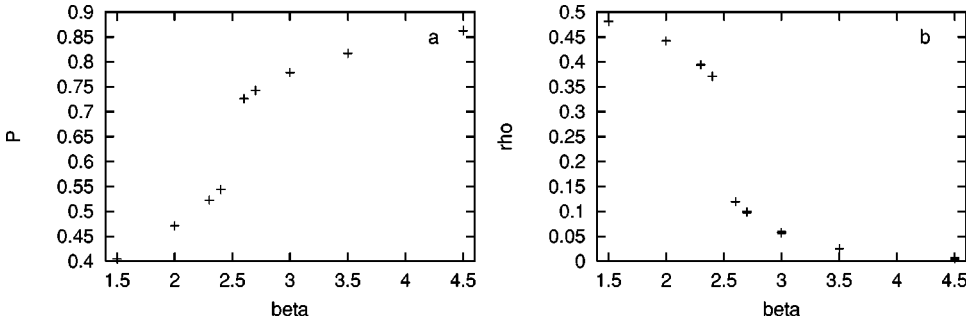


FIG. 1. (a) Plaquette square (P) and (b) $Z(2)$ monopole density (ρ), as a function of β_a . There is an abrupt rise in P and a fall in ρ , at $\beta_a \approx 2.5$.

been performed on all the links in the lattice. The link variables were updated by multiplying them with an $SU(2)$ element chosen at random from a table consisting of 50 elements which was biased to lie close to the unit element. The auxiliary Gaussian variables were updated by adding to them a number randomly chosen in the interval $(-cut, cut)$. The value of the cut was chosen so that an acceptance rate of around 40% was roughly maintained for both the updated variables. A finite temperature simulation is mimicked by choosing a lattice of small temporal extent, a large spatial extent, and periodic boundary conditions (with period β^{-1}) in the temporal direction. We have made our studies on lattices of different sizes. The maximum spatial size used was $N_\sigma = 10$ and the maximum temporal size was $N_\tau = 7$. Unless otherwise mentioned, the lattice size is usually $7^3 \times 3$.

We have decided to present our numerical results first along with some explanations, and only in the end do we start giving our interpretations. Though this may appear a bit tedious, there are some reasons for doing this. The numerical results are interesting in their own right and many of them are quite unexpected. Even before we discuss matters of interpretation, the numerical observations themselves present some puzzling features. The other reason for this approach is that the numerical results can always be considered separately from any physical interpretation we wish to attach to them; they can be regarded as empirical observations that have to be properly explained.

The observables that were studied were the plaquette square, the $Z(2)$ monopole density, the adjoint and fundamental Wilson line, the tiled Wilson line correlation function, and the auxiliary $Z(2)$ variable. We shall discuss these in turn. We shall use the terms small β_a and large β_a interchangeably with low temperature and high temperature respectively.

The $Z(2)$ monopole density and the plaquette square show an abrupt change at $\beta_a \approx 2.5$. Figure 1 shows the be-

havior of these two observables. The discontinuous jump in these quantities suggests a first order transition just as is observed in the bulk system. There is no indication of any other phase transition. The abrupt change in these observables signals a phase transition between the two regimes $\beta_a < 2.5$ and $\beta_a > 2.5$. The region $\beta_a < 2.5$ is a condensate of $Z(2)$ monopoles while the region $\beta_a > 2.5$ has virtually zero monopole density. Even the location of the phase transition, $\beta_a^{cr} \approx 2.5$, is very close to that observed in the bulk system ($\beta_a^{cr} \approx 2.6$).

We now come to the behavior of the Wilson line in the adjoint representation (L_a) which is the most interesting aspect of our studies. At low temperatures, it remains very small, but it jumps to a non-zero value at high temperatures. This jump occurs across $\beta \approx 2.5$ which is the same point where the plaquette square and the $Z(2)$ monopole density show a discontinuous behavior. The startling feature is that the adjoint Wilson line takes two distinct values at high temperatures. Depending on the starting configuration of the Monte Carlo run, the adjoint Wilson line takes either a positive or a negative value. A cold start (corresponding to an initial configuration where all the link variables are unity) always leads to the state with L_a positive, while a hot start (corresponding to a initial configuration where all the link variables are randomly distributed) usually leads to the state with L_a negative. The two metastable states are shown in Fig. 2(a). The reason why we call them metastable states will be explained later. In order to test whether these states are truly long lived metastable states the updating algorithm was tampered with in various ways, but these states always appeared. In fact, the *raison d'être* for simulating the action in Eq. (9) was to design an overrelaxation algorithm which could be used to verify these metastable states. Another surprising feature is that the average value of the plaquette square observable in both these metastable states appears to

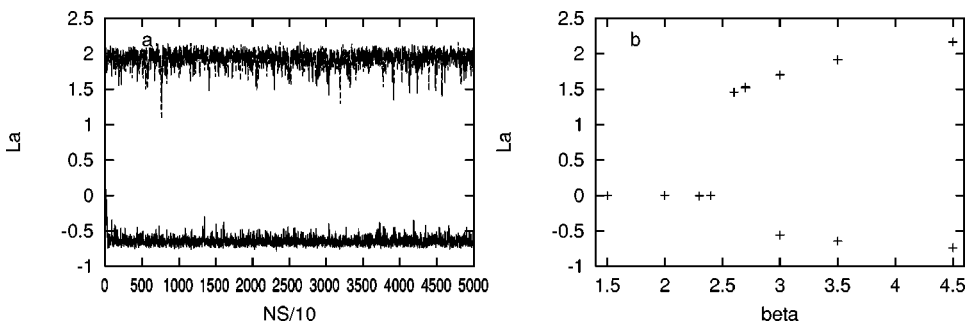


FIG. 2. (a) The two metastable states for L_a at $\beta_a = 3.5$. The positive value of L_a is reached after a cold start, and the negative value is reached after a hot start. (b) The variation of L_a with β_a .

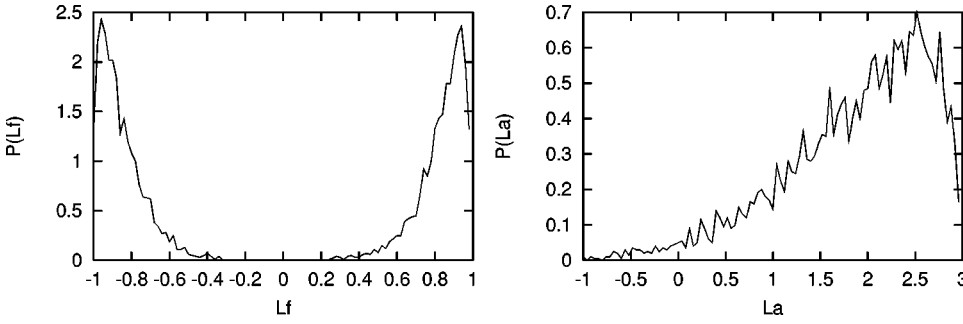


FIG. 3. The distribution of L_f and L_a in the L_a positive state. $\beta_a=3.5$.

be almost (but not exactly) equal. The value of the $Z(2)$ monopole density is extremely small at high temperatures and is not significantly different in these two metastable states. We also mention that we have hardly been able to see any tunnelings between these two metastable states except in a situation to be described later. A plot of L_a vs β_a is presented in Fig. 2b. At high temperatures, we show the values of L_a in both the metastable states which are observed in simulations.

Before accounting for these metastable states, we take a look at the distribution functions (normalized to 1) of the adjoint and fundamental Wilson line at high and low temperatures. They will help us to understand the structure of the high and low temperature states. We have plotted the single site distribution function because that gives more information about the configurations in these states. Figures 3 and 4 show these distributions for the the two high temperature states. In the state with L_a negative, there is a sharp peak at -1 while the state with L_a positive is peaked at a positive value (close to $+3$). We have already noted that the fundamental Wilson line will always have a zero expectation value because of the local $Z(2)$ symmetry. This requires

$$\langle L_f(x) \rangle = 0. \quad (18)$$

A zero expectation value can arise in different ways. Either the values of L_f can be peaked about zero or there can be two peaks at non-zero values symmetrically distributed about zero. The distribution of L_f in the two high temperature states shows that both these possibilities occur. The L_a positive state has double peaks symmetrically placed about zero; the L_a negative state has a sharp peak about zero. At low temperatures, the distribution of L_f is broadly peaked about zero. The distribution of L_a shows a peak at -1 but there is a tail stretching all the way to 3 . These are shown in Fig. 5. In Fig. 6 we also display similar distributions for the $SU(2)$

LGT at high temperatures. The distribution of L_a in the L_a positive state is very similar to its distribution in the high temperature phase of the $SU(2)$ LGT. At low temperatures, the distributions of L_f and L_a in the $SU(2)$ theory are very similar to those in the $SO(3)$ theory and so we do not present them. From these plots, the state with L_a positive in the $SO(3)$ LGT is seen to be quite similar to the high temperature (deconfined) phase of the $SU(2)$ LGT. The state with L_a negative is, of course, absent in the $SU(2)$ LGT. Let us now compare the distribution of the adjoint Wilson line in the L_a negative state with the low temperature, $L_a \approx 0$, state. Both profiles are peaked at $L_a \approx -1$, but there is a tail extending all the way to $+3$ in one, whereas in the other, the tail is truncated very sharply. A similar comparison of the L_f distribution shows that the two states differ only by the sharpness of their peaks centered on 0 . From the above observations, we conclude that although we see only one phase transition at $\beta_a \approx 2.5$, and this transition involves only the $Z(2)$ degrees of freedom, the distribution functions of the fundamental and adjoint Wilson line are sufficiently modified across the transition. The L_a negative state at high temperature and the low temperature state are quite similar in their configurations, which are peaked about $L_a = -1$; only the width of the distributions are different in the two cases. On the other hand, the L_a positive state has a peak at a different location. Likewise, the distribution of L_f in the low temperature phase differs from the one in the L_a negative state only by the width of its peak. In the L_a positive state, however, the L_f distribution is quite different and has two double peaks symmetrically placed about zero.

Another observable which can also be monitored is the average of the auxiliary plaquette variable. This observable is not gauge invariant and represents the additional $Z(2)$ degrees of freedom in the $SO(3)$ LGT. It is similar to L_f because it can arbitrarily flip its sign giving it a zero average value. Though its average value is always zero, its distribu-

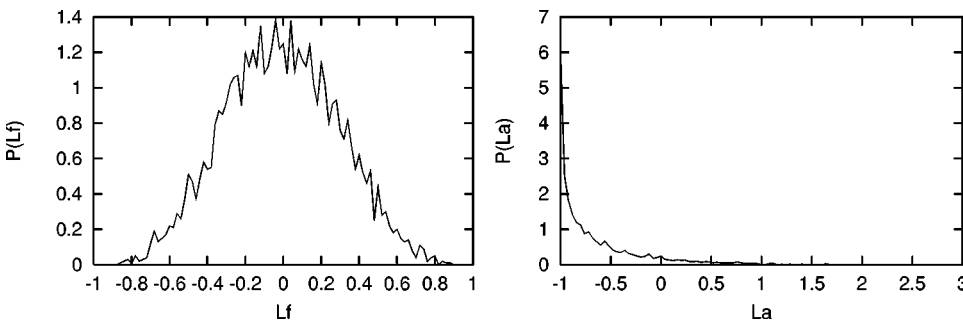


FIG. 4. The distribution of L_f and L_a in the L_a negative state. $\beta_a=3.5$.

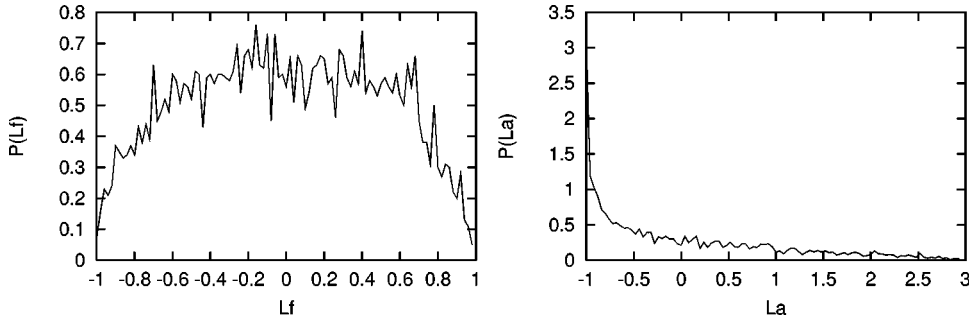


FIG. 5. The distribution of L_f and L_a in the low temperature phase. $\beta_a=2.0$.

tion undergoes a change across the transition just as L_f . This is shown in Fig. 7. At low temperatures, it has a broad peak centered on zero; at high temperatures, it has two peaks placed symmetrically about the origin. This means that the higher moments [like $\lambda(p)^2$ which is gauge invariant] will show a discontinuous behavior across the transition.

Now we turn to another aspect of our numerical results. We had mentioned earlier that in the states with L_a negative and L_a positive, the values of observables such as the plaquette square and the $Z(2)$ monopole density were almost equal. This should be checked for different values of β_a and N_τ . On an $N_\tau=3$ lattice, the two states have the same value of the plaquette square observable for a wide range of couplings. The differences between the two states start showing up only at very large couplings. We plot the time evolution (Fig. 8) of the plaquette square observable for these two metastable states on an $N_\tau=3$ lattice for two different couplings, 8.5 and 10.5. We notice that the two values start moving apart only after $\beta_a=8.5$. The same feature is observed when we go to lattices of temporal size $N_\tau=2$. This means that at very high temperatures (large β_a or small N_τ), the L_a positive and L_a negative states begin to differ slightly from each other at least in the values of the plaquette square observable (which is the energy density in a bulk system).

The tiled Wilson line correlation function also behaves differently at low and high temperatures. At low temperatures, it falls rapidly to zero at large distances; in the two high temperature phases, it again behaves differently; in the L_a positive state, it reaches a non-zero value at large distances, and in the L_a negative state, it falls to zero at large distances just as in the low temperature phase. This is shown in Fig. 9. This measurement of the correlation function was done on a $10^3 \times 3$ lattice. Some simple arguments can be given for this behavior of the tiled Wilson line correlation function. At strong coupling, it is natural to expect the tiled Wilson line correlation function to have an area law. This

translates into a rapid fall of the correlation function. At high temperatures, a different argument can be made. The very small (virtually zero) $Z(2)$ monopole density means that virtually all the cubes in the lattice satisfy

$$\sigma(c) = +1. \quad (19)$$

This condition can be satisfied by

$$\lambda(p) = |\lambda| \prod_{l \in \partial p} z(l). \quad (20)$$

The extra $Z(2)$ variables [$z(l)$] that occur on the Wilson line correlation function can be absorbed in the Haar invariant measure, and the Wilson line correlation function reduces to the correlation function of two fundamental Wilson lines, apart from some normalization factors that arise because of the absolute value of the $\lambda(p)$ variables. Since the extra $Z(2)$ variables can be absorbed away, the action of the $SO(3)$ LGT reduces to that of the $SU(2)$ LGT. In the $SU(2)$ LGT, at high temperatures, the correlation function of two fundamental Wilson lines approaches a non-zero value at large distances. This is precisely the behavior seen for the tiled Wilson line correlation function in the L_a positive state.

So far the results were for asymmetric lattices. We now record some observations on symmetric lattices. In the infinite lattice size limit, a symmetric lattice corresponds to the bulk zero-temperature system. However, simulations are always done on finite lattices. A finite symmetric lattice can also be regarded as a finite temperature system whose spatial volume is small (since $N_\sigma \approx N_\tau$). When the spatial volume is small, the tunneling probability between metastable states will increase [since it goes as $\exp(-\alpha V)$ where α is some positive constant and V is the volume]. The simulations on a symmetric lattice are more likely to see tunnelings between

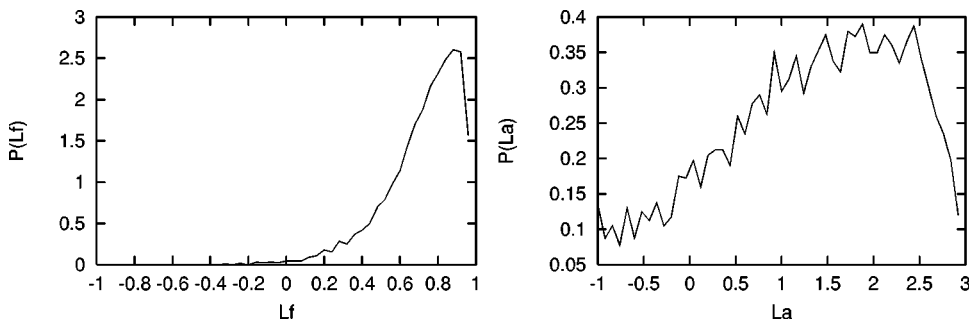


FIG. 6. The distribution of L_f and L_a in the high temperature phase of the $SU(2)$ theory. $\beta_f=4.5$.

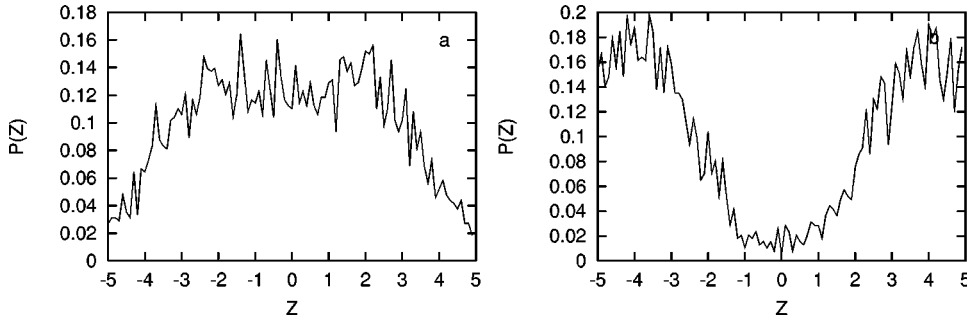


FIG. 7. The distribution of $\lambda(p)$ (called Z in the figure) in the (a) low and (b) high temperature phases.

metastable states and this is indeed the case. For large β_a (3.5), the state with L_a negative also appears whenever the simulation is begun from a hot start. The state with a cold start rarely settles down to a steady value and oscillates as shown in Fig. 10. This behavior occurs for many couplings (and seeds of the random number generator) and is not a feature of any particular run or updating algorithm. Also it occurs only for large symmetric lattices and is never observed on, for instance, an $N_\tau=3$ lattice. It is natural to interpret this oscillation as tunneling between degenerate or almost degenerate metastable states. If this is indeed the case, we can study the tunneling probability between these states. This suggests a small experiment. So far, the temporal extent of the lattice was kept fixed at $N_\tau=3$ and the temperature was varied by varying β_a . We now fix β_a and vary N_τ . This has the effect of varying the temperature at a fixed coupling (which can be chosen to be large). The reason for doing this is as follows: fixing β_a and varying N_τ not only has the effect of varying temperature, but if N_σ is kept fixed, it also has the effect of achieving a simulation in a small volume. This will aid tunnelings between metastable states which are degenerate or almost degenerate. We choose two values of β_a ; they are 3.5 and 8.5. The purpose of this exercise is to see how the tunneling probabilities are affected as one increases the temperature. We find it convenient to plot the distribution function of L_a (now this refers to the value of the adjoint Wilson line averaged over all lattice sites) as a function of N_τ (β^{-1}). This evolution is shown in Fig. 11. On lattices of large temporal extent, one sees two peaks in the distribution of L_a and these are centered on positive and negative values. One notices a gradual movement of density from the L_a negative region to the L_a positive region as N_τ is decreased. For $N_\tau=4$, the two peaks have disappeared and there is only a single peak over the L_a positive state. This same experiment is repeated in Fig. 12 for a higher coupling (8.5) and one again observes a move-

ment of density from the L_a negative region to the L_a positive region, but this time the transition to a single peak occurs at a larger value of N_τ ($N_\tau=5$). This suggests that the L_a positive state appears at higher values of N_τ for larger values of β_a . The above distributions were plotted after gathering data from 50000 iterations. We have also studied the densities of L_f at a single site as the temperature is increased and we again observe the shape changing from a single peak centered on zero to a double peak symmetrically distributed about zero [15,20].

Finally we wish to make a few remarks about the shift in the critical value of β_a as a function of N_τ . The bulk transition moves to $\beta_a \approx 2.4$ on an $N_\tau=2$ lattice and is at $\beta_a \approx 2.52$ on a $N_\tau=3$ lattice. We have not observed any significant shift on an $N_\tau=4$ lattice.

This concludes our numerical studies of the $SO(3)$ LGT. Before we interpret our numerical results, we would like to point out an important relation between the couplings of the $SU(2)$ and the $SO(3)$ LGT at weak coupling. The relation between β_f and β_a when both are large is

$$\beta_f = \frac{8}{3} \beta_a. \quad (21)$$

This relation is true in the naive classical limit and does not represent the effects of all the quantum corrections but it is still a good guide to the weak coupling behavior of the $SU(2)$ and the $SO(3)$ LGTs. If there is a deconfinement transition in the $SO(3)$ LGT at a large coupling, which is separated from the bulk transition, it must occur at $\beta_a > 2.6$. This means that the corresponding transition in the $SU(2)$ LGT must occur at $\beta_f > 5.6$ (assuming that the weak coupling relation is approximately valid at these couplings). Simulations in [17] have shown that $\beta_f^{cr} = 2.76$ on a $N_\tau = 16$ lattice. This would mean that deconfinement transitions

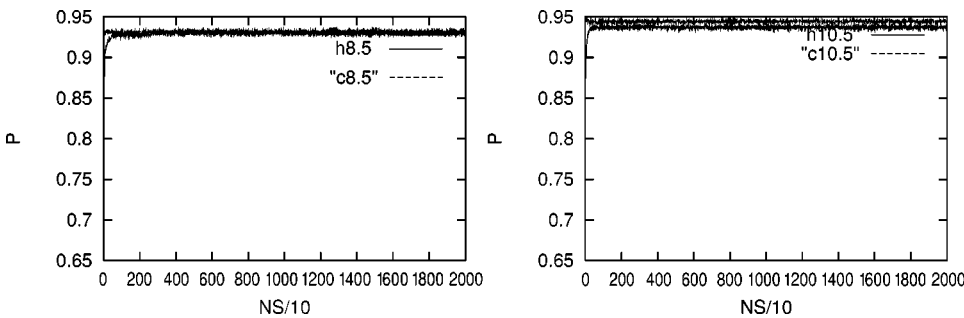


FIG. 8. Plaquette square evolving with Monte Carlo sweeps. The values of β_a are (a) 8.5 and (b) 10.5.

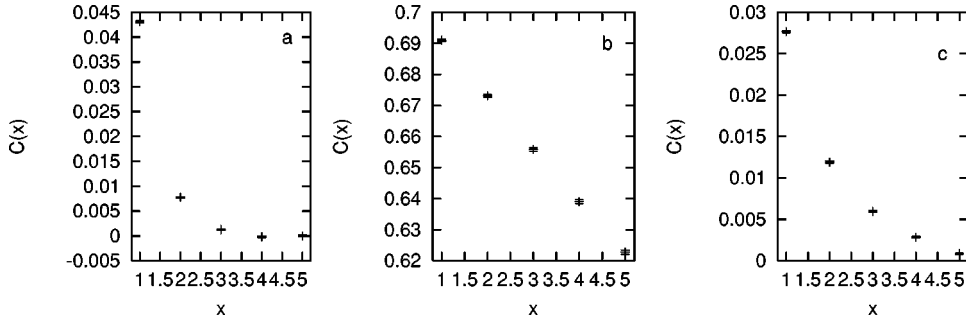


FIG. 9. The tiled Wilson line correlation function in the (a) L_a negative phase, (b) L_a positive phase, and the (c) low temperature phase. $\beta_a = 3.5$ in (a) and (b) and $\beta_a = 2.0$ in (c).

in the $SO(3)$ LGT require very large temporal lattices. Such large temporal lattices correspond to very low temperatures (in lattice units).

We will now gather together all our numerical observations and try to tie them up to arrive at a consistent physical picture. We will find that this presents several difficulties and that we are faced with many possibilities. The discontinuous behavior of the plaquette square and the $Z(2)$ monopole density at $\beta_a \approx 2.5$ appears to be a replica of the transition in the bulk system. It looks as if finite temperature effects hardly shift the $Z(2)$ transition. As this transition is so similar to the bulk transition, we expect that only the $Z(2)$ degrees of freedom are changing across it. Hence we expect the confining properties of the gauge theory to be unchanged across this transition. That the two phases differ by a distribution of the $Z(2)$ degrees of freedom is also clear from Fig. 13. These observations are also in line with the studies made in [8].

We now come to the behavior of the adjoint Wilson line which is the most striking aspect of our numerical results. At low temperatures, the adjoint Wilson line has a very small numerical value (in fact it is very close to zero all the way until the transition). This small value at low temperatures is quite unexpected because a static quark in the adjoint representation can always bind with a gluon and form a state of finite energy. Though we expect the adjoint Wilson line to be always non-zero, there is no reason why it should take such a small value at low temperatures. Nonetheless, in the strong coupling approximation,

$$\langle L_a \rangle \approx (\beta_a/3)^{4N_\tau}, \quad (22)$$

and is quite small on the lattices that we are using. This explains the small value of L_a in the strong coupling region though it does not provide a reason why L_a should be small all the way until the phase transition. The adjoint Wilson line taking two distinct values at high temperatures is the most unexpected feature of our results. Equally puzzling is the

observation that observables such as the plaquette square appear to take almost the same values in these two states. This behavior is very reminiscent of the high temperature phase of the $SU(2)$ LGT in which one observes metastable states which are related by a $Z(2)$ transformation. In the $SU(2)$ LGT, the global $Z(2)$ symmetry ensures that the two states have the same free energy. In the $SO(3)$ LGT, there is no obvious symmetry relating the L_a positive and L_a negative states; the presence of two degenerate minima in the free energy in the absence of any such symmetry would be quite a remarkable instance. Moreover, although the physical interpretation of the L_a positive state is quite clear—it is similar to the deconfined phase of the $SU(2)$ LGT—the L_a negative state does not easily admit a physical interpretation. However, as both these states seem to appear immediately after the bulk transition, we are led to the different possibilities considered by [10] in their studies of the mixed action $SU(2)$ lattice gauge theory. These include (i) only bulk transition and no deconfinement transition, (ii) only deconfinement transition and no bulk transition, and (iii) two transitions with a separation which we are unable to resolve with our numerical methods. Possibility (i) goes against many theoretical and numerical arguments favoring a deconfinement transition at high temperatures. Possibility (ii) requires the transition to be of second order according to the arguments in [5]. It also requires the transition point to shift as the temporal lattice size is increased. We have not noticed any significant shift in the critical coupling from $N_\tau = 3-4$. Though we do not have a proof for any of these possibilities, the third possibility seems to be the least dramatic of the three. Before proceeding further to interpret our numerical results, we take the point of view that the presence of the L_a negative state is quite significant and has to be properly accommodated in any scheme. Though the physical interpretation of the L_a positive state is quite clear, the L_a negative state still needs to be explained.

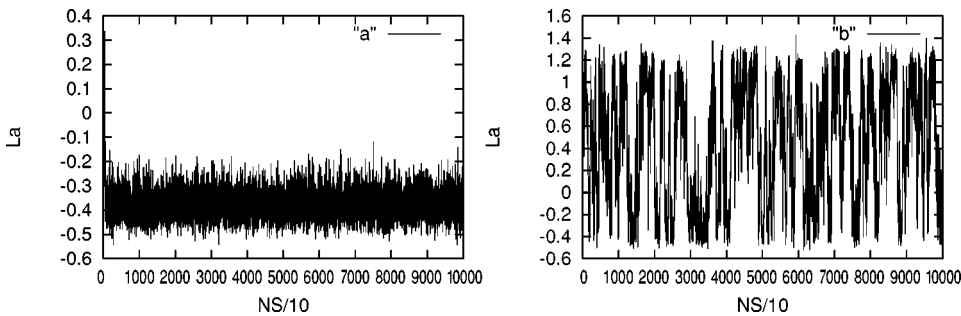


FIG. 10. L_a on a 7^4 lattice as a function of Monte Carlo sweeps for (a) hot start and (b) cold start. $\beta_a = 3.5$.

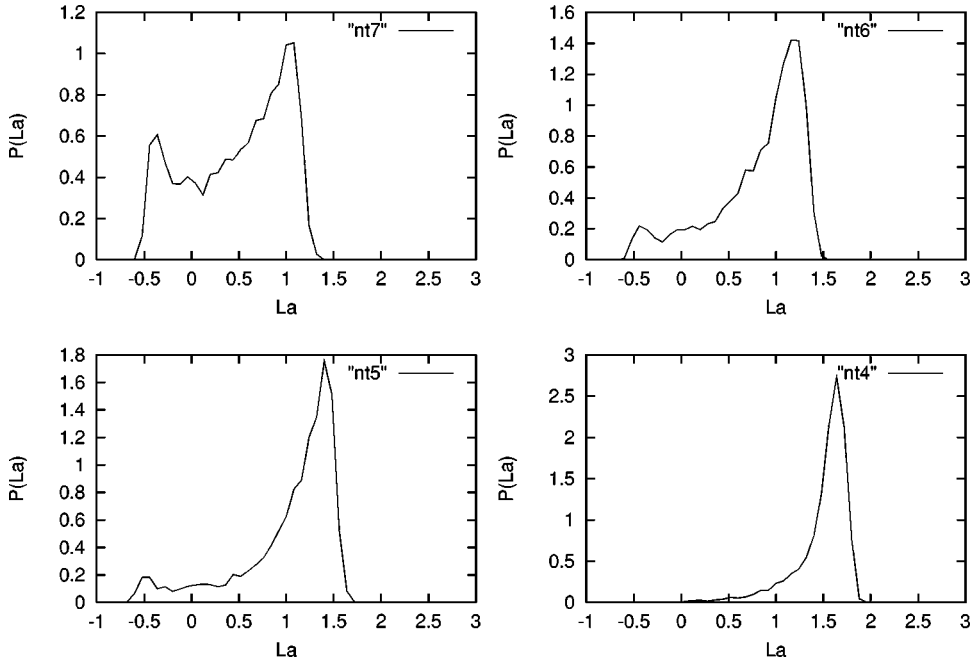


FIG. 11. The distribution of L_a as a function of N_τ at $\beta_a=3.5$.

Let us examine two possible interpretations. One possible interpretation is that we have only the bulk transition driven by the $Z(2)$ monopoles. As we have observed only one transition, and the states with L_a positive and L_a negative appear immediately after this transition, this may seem quite a promising explanation. One may also think that these two states are physically equivalent. A recent measurement in [18] of the correlation length of the adjoint Wilson line came up with the result that it was the same in the two states. This seems to support the picture of two distinct but physically equivalent states. Nevertheless, this interpretation does have its problems. Our studies of the plaquette square observable and the tiled Wilson line correlation function show that these two observables behave differently in the two states. Apart

from the slightly different numerical values of the plaquette square operator in these two states (which measures the energy density in the bulk system), the tiled Wilson line correlation function differs drastically in the L_a positive state and the L_a negative state. Moreover, the exact physical equivalence of these states, in the absence of a symmetry relating the two, would be quite a remarkable instance. We have not been able to discover any symmetry that maps the L_a positive state to the L_a negative state and which leaves the action invariant. In the absence of such an explicit symmetry transformation, we cannot be sure that there does indeed exist such a transformation. The phase diagram of the $SO(3)$ LGT at non-zero temperature in this scenario, where there is only a single bulk transition, would be as in Fig. 13 without the

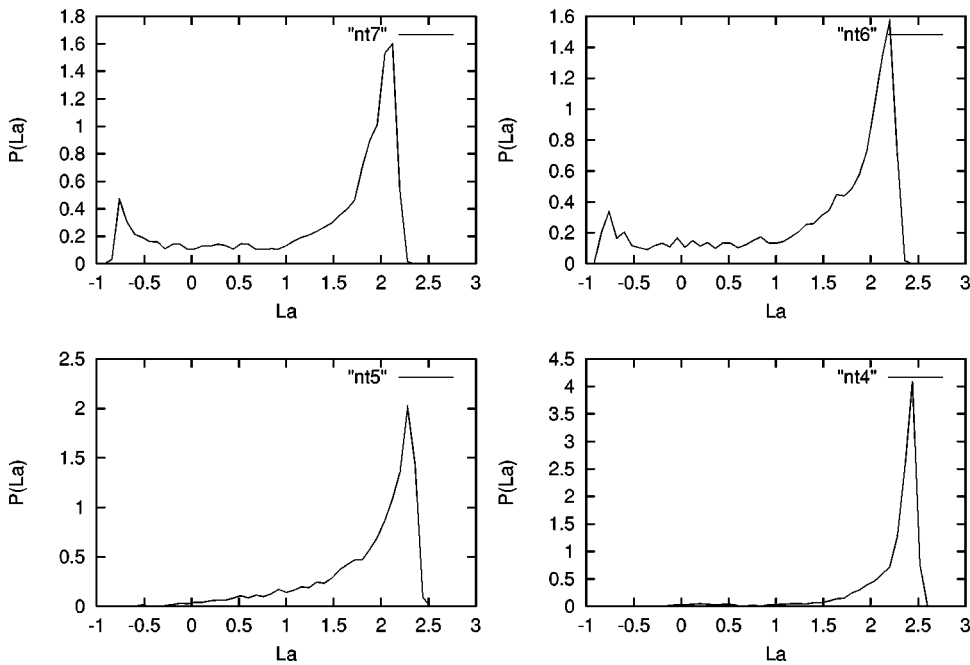


FIG. 12. The distribution of L_a as a function of N_τ at $\beta_a=8.5$.

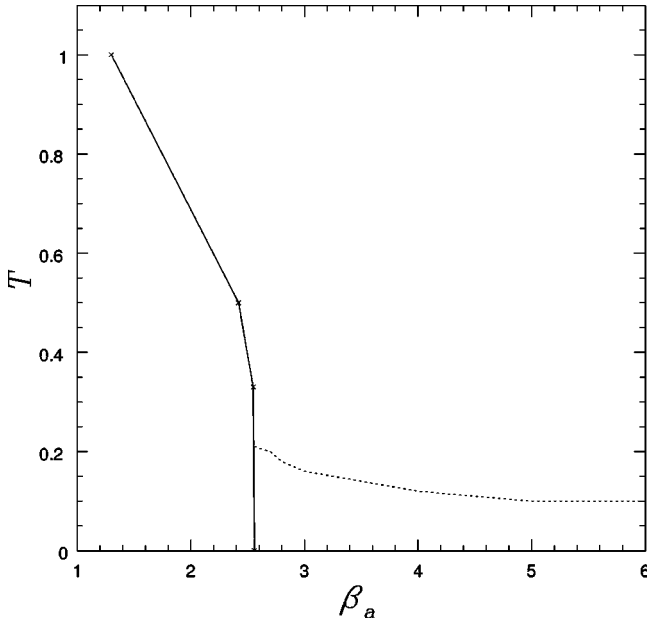


FIG. 13. Possible phase diagram of the $SO(3)$ LGT at finite temperature. The solid line is the bulk transition. The dotted line is the deconfinement transition.

dotted line. There is only the bulk phase transition which is driven by the $Z(2)$ monopoles.

The other interpretation is that the states with L_a positive and L_a negative are physically quite different. From a numerical standpoint, this seems to be supported by our observations of the plaquette square observable and the tiled Wilson line correlation function, both of which behave differently in these two states. Also, a comparison of the distributions of L_a at high and low temperatures suggests that the L_a negative state and the $L_a \approx 0$ (which is the low temperature confining phase) state are structurally similar, apart from the width of their distribution functions (of L_a and L_f). Our observations on symmetric lattices also suggest that this state can be associated with the bulk system. A study of the tunneling probabilities indicated that there was a passage from the L_a negative region to the L_a positive region as we increased the temperature. This would suggest that the L_a negative state is associated with the bulk (confining) phase which passes into a deconfining phase at high temperatures. The tiled Wilson line correlation function also has the same behavior in the low temperature phase and the L_a negative state. An important consequence of this interpretation is the existence of a phase transition between the bulk phase and the deconfined phase at large couplings, which is quite different from the $Z(2)$ transition. Let us mention some of the questions raised by this picture. If the two states are physically very different, why is it that they always seem to appear together? Within our present analysis we cannot answer this question satisfactorily but it is possible that there are two minima in the effective potential at high temperatures which are closely spaced, and this causes the configurations to get trapped in one of the two, almost degenerate, minima. Also, we should emphasize that it is only the cold start that always ends up in the L_a positive state; a hot start usually ends up in

the L_a negative state. A cold start (in which the initial L_a is $+3$) is already close to the L_a positive state and always reaches that state. A hot start, on the other hand, corresponds to $L_f \approx 0$ and usually settles to the L_a negative state. If the effective potential has two minima of different depths, then even a local minimum can appear as a very long lived metastable state. Such examples are known to occur in spin glass systems. Since our updating algorithm is a local algorithm, it will find it difficult to move the system away from a local minimum. Moreover, if there is no symmetry connecting these two minima, it is difficult to make global updates (such as flipping of all the spins) which move the system from one minimum to the other. A mean field analysis [19] by one of the authors (S.C.) shows that the L_a negative state persists as a local minimum, even at high temperatures, and this may explain its appearance in simulations even at large couplings. Though we have not been able to directly detect a phase transition at large coupling, our observations of tunneling probabilities on lattices of large N_τ show that there is a passage from a double peak structure to a single peak structure at high temperatures. The argument after Eq. (21) also tells us that the search for this transition has to be carried out at very low temperatures (large temporal lattices). In this picture, the phase diagram of the $SO(3)$ LGT would be as in Fig. 13. The solid line is the $Z(2)$ driven transition which, at least on an $N_\tau=3$ lattice, is a first order transition. At zero temperature, both sides of the transition are confining phases and at a non-zero temperature both phases undergo transitions to a common high temperature phase. The dotted line is the location of the phase transition from the bulk phase to the deconfined phase. This line lies very close to the β_a axis as the transition temperature is quite low. At large β_a , the line will be similar to the line in the $SU(2)$ LGT as is expected from the universality of lattice actions. We consider this scenario to be more plausible, taking into consideration our numerical results and theoretical expectations.

We now wish to discuss some theoretical issues which have an important bearing on the interpretation of our results. It can be shown that the expectation value of the adjoint Wilson line is always a non-negative quantity. This basically follows from the fact that a static source in the adjoint representation can always form a bound state with a gluon and give a positive contribution to the partition function. In fact, the free energy interpretation of the average value of the adjoint Wilson line in Eq. (16) presupposes that it is always a non-negative quantity. However, we seem to be getting negative values in simulations. The fundamental Wilson line in the $SU(2)$ LGT also takes positive and negative values. For the fundamental Wilson line, one gets around this contradiction by saying that it is the correlation function of two Wilson lines which can be given the physical interpretation of measuring the free energy of a quark-antiquark pair [21]. This correlation function is always positive and there is no problem with the free energy interpretation. The average value of an isolated fundamental Wilson line on a finite lattice is in principle always zero, because tunneling between the two metastable states always restores the symmetry; individual Wilson lines are measured in simulations for purely operational reasons. The same avenue is not open for the

adjoint Wilson line. Even an isolated adjoint Wilson line can be non-zero, and it is always a non-negative quantity. This seems to contradict the observations made in simulations in which we have observed negative values for the adjoint Wilson line. The way out is that in finite systems, there will always be tunnelings (though one may have to wait a very long time) between the metastable states (which in this case are not connected by any symmetry). In the $SO(3)$ LGT, the tunnelings are between the L_a positive and the L_a negative states, and since these states are non-uniformly distributed about zero, they can give a net positive value for the average of L_a . This is clearly seen in Fig. 11 and Fig. 12 where the distributions of L_a ensure that the mean value of L_a is always in the positive region. The reason why we have called the states observed in numerical simulations as metastable states is that their thermodynamic significance is not obvious. Though we observe states having a positive and a negative value of L_a in numerical simulations, the average value of L_a is got by averaging over these two metastable states. In the thermodynamic limit, the value of $\langle L_a \rangle$ in any phase is always a non-negative quantity. If there is a phase transition at high temperatures, the observable that detects the transition is L_a . Figure 11 shows that average of L_a need not change discontinuously even though there is a multiple peak structure for L_a across the phase transition. This is because the mean value of L_a (which is always a positive quantity) gradually increases as the temperature is increased. We now make a few remarks about the continuum limit. Apart from the thermodynamic limit, one also has to take the continuum limit so that the lattice system goes over to some physical system (in this case, Yang-Mills theory). This requires taking the simultaneous limits, $N_\tau \rightarrow \infty$ and $a \rightarrow 0$, and the passage to this limit can also affect the physical properties of the lattice system; the order of the phase transition can also change as we approach the continuum limit and may even become second order. The possibility of a second order phase transition in the continuum limit is also indicated by the fact that the absolute value of the adjoint Wilson line decreases as the temporal lattice size is increased. Thus, the multiple peaks seen in the adjoint Wilson line will move

closer to each other on very large temporal lattices. We conjecture that in this limit, these distributions will resemble the corresponding distributions in the $SU(2)$ LGT.

In this paper we have mainly emphasized the numerical results of our studies of the $SO(3)$ LGT. We have observed a deconfining phase at high temperatures which is just like the deconfining phase of the $SU(2)$ LGT. As there is no global $Z(2)$ symmetry operating in this model, this is a deconfining phase without any symmetry breaking as in the $SU(2)$ LGT. We have also observed the bulk transition which is driven by the $Z(2)$ degrees of freedom. In the course of our studies, we have stumbled into a new metastable state which would have been *a priori* very difficult to guess. The incorporation of this new state in the model presents us with several difficulties, and a reconciliation of the numerical observations with our physical intuition leads us to consider different scenarios. We have pointed out two possible scenarios for the phase diagram of the $SO(3)$ LGT. Both of them are able to explain some of the observations made in simulations, but they also pose problems for a complete reconciliation between numerical observations and physical expectations. Our analysis does show, however, that the $SO(3)$ LGT has a much richer behavior than the $SU(2)$ LGT. It is quite likely that these features persist in systems which have bulk transitions and which are also expected to have finite temperature deconfinement transitions.

One of the authors (S.C.) has tried to make some analytical calculations in order to explain the puzzling features of the $SO(3)$ LGT [19]. A mean field analysis of the $SO(3)$ LGT reveals the presence of the L_a negative and L_a positive states at high temperatures. The structure of the metastable states in simulations, at high and low temperatures, can also be explained by the mean field theory. The mean field theory analysis also predicts the existence of a phase transition at large β_a for the $SO(3)$ LGT [19].

ACKNOWLEDGMENTS

One of the authors (S.C.) would like to acknowledge useful discussions with Rajiv Gai and Saumen Datta.

-
- [1] J. Engels, F. Karsch, H. Satz, and I. Montvay, Phys. Lett. **101B**, 89 (1981); J. Engels, F. Karsch, H. Satz, and I. Montvay, Nucl. Phys. **B205**, 545 (1982); H. Satz, *ibid.* **B252**, 183 (1985); J. Engels, J. Fingberg, F. Karsch, D. Miller, and M. Weber, Phys. Lett. B **252**, 625 (1990); J. Engels, F. Karsch, and K. Redlich, Nucl. Phys. **B435**, 295 (1995); C. Boyd, J. Engels, F. Karsch, E. Laermann, C. Legeland, M. Lutgemeier, and B. Petersson, *ibid.* **B469**, 419 (1996).
- [2] A. Polyakov, Phys. Lett. **72B**, 477 (1978); L. Susskind, Phys. Rev. D **20**, 2610 (1979).
- [3] J. Kuti, J. Polonyi, and K. Szlachanyi, Phys. Lett. **98B**, 199 (1980); L. McLerran and B. Svetitsky, *ibid.* **98B**, 195 (1980).
- [4] K. G. Wilson, Phys. Rev. D **10**, 2445 (1974).
- [5] L. Yaffe and B. Svetitsky, Nucl. Phys. **B210**[FS6], 423 (1982); L. McLerran and B. Svetitsky, Phys. Rev. D **26**, 963 (1982); **24**, 450 (1981); B. Svetitsky, Phys. Rep. **132**, 1 (1986).
- [6] R. Gai and H. Satz, Phys. Lett. **145B**, 248 (1984); J. Engels, J. Jersak, K. Kanaya, E. Laermann, C. B. Lang, T. Neuhaus, and H. Satz, Nucl. Phys. **B280**, 577 (1987); J. Engels, J. Fingberg, and M. Weber, *ibid.* **B332**, 737 (1990); J. Engels, J. Fingberg, and D. Miller, *ibid.* **B387**, 501 (1992).
- [7] K. Kajantie, C. Montonen, and E. Pietarinen, Z. Phys. C **9**, 253 (1981); T. Celik, J. Engels, and H. Satz, Phys. Lett. **125B**, 411 (1983); J. Kogut, H. Matsuoka, M. Stone, H. W. Wyld, S. Shenker, J. Shigemitsu, and D. K. Sinclair, Phys. Rev. Lett. **51**, 869 (1983); J. Kogut, J. Polonyi, H. W. Wyld, J. Shigemitsu, and D. K. Sinclair, Nucl. Phys. **B251**, 318 (1985).
- [8] I. G. Halliday and A. Schwimmer, Phys. Lett. **101B**, 327 (1981); **B102**, 337 (1981); R. C. Brower, H. Levine, and D. Kessler, Nucl. Phys. **B205**[FS5], 77 (1982).

- [9] G. Bhanot and M. Creutz, Phys. Rev. D **24**, 3212 (1981).
- [10] R. Gai, M. Mathur, and M. Grady, Nucl. Phys. **B423**, 123 (1994); R. V. Gai and M. Mathur, *ibid.* **B448**, 399 (1995).
- [11] T. Blum, C. DeTar, U. Heller, L. Karkkainen, K. Rummukainen, and D. Toussaint, Nucl. Phys. **B442**, 301 (1995).
- [12] S. Elitzur, Phys. Rev. D **12**, 3978 (1975).
- [13] P. H. Daamgard, Phys. Lett. B **183**, 81 (1987); **194**, 107 (1987); J. Fingberg, D. Miller, K. Redlich, J. Seixas, and M. Weber, *ibid.* **248**, 347 (1990).
- [14] J. Kiskis, Phys. Rev. D **51**, 3781 (1995).
- [15] C. Srinath, Ph.D. thesis, 1996.
- [16] M. Faber *et al.*, Vienna report, 1986.
- [17] J. Fingberg, U. Heller, and F. Karsch, Nucl. Phys. **B392**, 493 (1993).
- [18] S. Datta and R. Gai, Phys. Rev. D **57**, 6618 (1998).
- [19] S. Cheluvvaraja, Report No. TIFR-TH-98-36.
- [20] S. Cheluvvaraja and H. S. Sharatchandra, hep-lat/9611001.
- [21] J. Kiskis, Phys. Rev. D **41**, 3204 (1990).